Water Resources Management (2024) 38:1773–1790
https://doi.org/10.1007/s11269-024-03765-4

Investigating the Non-Linear Effects of Breach Parameters on a Dam Break Study

Hasan Oğulcan Marangoz[1] · **Tuğce Anılan**[2] · **Servet Karasu**[3]

Received: 3 November 2023 / Accepted: 22 January 2024 / Published online: 6 February 2024

Abstract
When settlements are located close to a dam, it is important to accurately predict the breach peak flow and the time to reach the peak. Therefore, the prediction of dam breach properties is essential in dam break studies. Dam breach parameters such as the breach side slope, final bottom width, final bottom elevation, weir coefficient, breach formation time, and initial elevation of reservoirs are the key variables for estimating the peak discharge during a dam break scenario. In this study, these six breach parameters were analyzed to investigate the impact of breach parameters on breach peak flow and the time to reach the peak. Thus, several scenarios were calculated and compared for Atasu Dam. The results revealed that the role of the initial water elevation, final bottom elevation, and breach development time had more of an impact on the breach peak flow and the time to reach the peak. In addition, the study indicated that the final bottom width and breach weir coefficient were less sensitive to both the peak discharge and peak discharge time. Furthermore, the analysis indicated that the breach side slope parameter had no major influence on the time to peak while also having an insignificant impact on the peak discharge. Understanding this breach mechanism provides a basis for relevant research in designating key parameters for dam break analysis. Thus, the results can contribute to decision making toward the design of flood mitigation and dam emergency action planning.

Keywords Dam break · Breach parameters · Breach peak flow · Time to peak

✉ Tuğce Anılan
tugcekoc@ktu.edu.tr

Hasan Oğulcan Marangoz
hasanogulcan@gmail.com

Servet Karasu
skarasu@beun.edu.tr

[1] Faculty of Engineering & Architecture, Department of Civil Engineering, Recep Tayyip Erdoğan University, 53100 Rize, Turkey

[2] Faculty of Engineering, Department of Civil Engineering, Karadeniz Technical University, 61080 Trabzon, Turkey

[3] Faculty of Engineering, Department of Civil Engineering, Zonguldak Bülent Ecevit University, 67100 Zonguldak, Turkey

1 Introduction

Floods are considered one of the most common devastating natural hazards in terms of life and property loss (Anılan and Yüksek 2017). Some of the most damaging flash flood events worldwide are associated with dam breaches (also widely called dam breaks), which release a large amount of water to downstream areas, thus endangering not only human life, but also the economy, damaging structures, and causing the destruction of the natural environment/ecosystems (Psomiadis et al. 2021; Yudianto et al. 2021; Garoosi et al. 2022). Therefore, it is important to understand the mechanics of the break process in a dam collapse in order to prepare dam break-induced flood–wave inundation maps, as well as to identify high-hazard zones so as to create emergency plans (Peng et al. 2021; Li et al. 2021; Karim et al. 2021; Zali et al. 2021).

Dam breaches can be triggered by natural factors or human activities such as earthquakes, overtopping, flooding exceeding the designed level, insufficient capacity of spillways or reservoirs, piping, military destruction, dam foundation failure, or poor-quality construction (Karim et al. 2021; Ramola et al. 2021; Yudianto et al. 2021). In recent years, the probability of dam breaches caused by extreme weather due to global climate change has also greatly increased (Li et al. 2021). Due to the geometric, hydraulic, natural factors, and complexity of the nonlinear rapidly varied unsteady flow regime, the theoretical solution is still limited to a few simple problems (Garoosi et al. 2022). Therefore, there is always a risk of devastating damage (Özmen-Çağatay et al. 2022).

For many years, many analytical, numerical, statistical, and experimental models have been constructed for dam break-induced flood–wave propagation, and they are widely used in flood risk mapping (Turhan et al. 2019; Zali et al. 2021; Özmen-Çağatay et al. 2022). Many researchers have developed numerical models that were calibrated and verified against experimental and field data (Tingsanchali and Chinnarasri, 2001; Shen et al. 2020; Wang et al. 2022). Certain studies have focused on assessing the risk of dam overtopping failure probability via statistical processes (Zhang and Tan 2014; Liu et al. 2018; Sarchani and Koutroulis 2022). Various studies have utilized empirical equations to estimate the peak breach discharges and breach parameters (Haltaş et al. 2016; Říha et al. 2020), while others have examined the uncertainty of breach parameters through stochastic modeling (Bellos et al. 2020). Numerical model studies have been performed in both one-dimensional (1D) and two-dimensional (2D) models (Haltaş et al. 2016; Marangoz and Anılan 2022). During the last two decades, due to the rapid development of computer power and mathematical algorithms, the application of CFD as a promising alternative to analytical methods has become more important and widespread (Garoosi et al. 2022). Peng et al. (2023) carried out a three-dimensional (3D) numerical analysis of a dam break event by using the volume-of-fluid method and various turbulence modeling approaches. They also verified their results with the experimental data of a previous study. Khoshkonesh et al. (2023) also used a CFD package for a 3D dam break analysis. They used the model for estimating the flow characteristics during a dam failure for various conditions.

Most of the previous studies have focused on the basic hydraulic features, including the depth, discharge, and velocity, but they did not consider the dynamics of the interaction between the breach parameters and flow hydrograph (Lee 2019; Sarchani and Koutroulis 2022; Marangoz and Anılan 2022). Determining which parameters are the most critical and which ones are negligible still requires more investigation. The results of this study demonstrate that the breach parameters should be ordered according to their relative influence on flood peak hydrographs and the time to reach the peak.

To understand the impact of the breach parameters on these aspects, 6 of the most common breach parameters were selected and 36 scenarios were examined. A mathematical system was built to investigate the parameter-based effects. An accurate prediction of breach characteristics has practical significance for providing people with early warnings, thus enabling more successful emergency evacuations, which reduce life loss and property damage.

2 Breach Modeling Procedure

A breach can be defined as a small cut or crack in a dam body that can initiate a dam failure process, which thus leads the reservoir water to move downstream of the dam with full velocity (Yi 2011). All failure events start with a breach initiation process. The dam break-induced flood hydrograph properties and flow properties primarily depend on the breach geometry and breach formation time (Peter et al. 2018; Ramola et al. 2021). Breach parameters can be grouped according to their characteristics: (i) geometric parameters (the width of the breach, the slopes of the breach, and the final height of the breach); (ii) time-related parameters such as breach formation time; and (iii) parameters that characterize the breach flow (the discharge coefficient, the height of the breach, the tolerable height of the water before a failure occurs, the weir coefficient, and the height where internal erosion begins) (Bellos et al. 2020; Bello et al. 2022). Many of these variable combinations can be found in field conditions, thus resulting in different scenarios. Breach depth is usually taken to be the dam height, and some argue that the breach side slope angle should be taken as vertical for most cases; as such, the breach width and breach formation time are the two parameters of most interest (Wahl 2010). Froehlich (2008) reported that there may also be uncertainties regarding breach properties. In dam break simulation models, the user is required to estimate the breach geometry and dimensions independently and provide this information as an input to the simulation model. The uncertainties of these dam breach models are often quantified in terms of prediction errors, which are minimized during model calibration by selecting appropriate data and fitting procedures (Peter et al. 2018).

The dam breach models available in the literature can be classified as follows: (1) empirical models, (2) parametric-based models, (3) physical-based breach models, and (4) statistical models. Empirical models are widely used in dam breach analysis as they are easier to use for estimating breach parameters. Parametric-based models are also generally simple; however, their accuracy of prediction is questionable. The physical-based models are more complicated to implement structurally, but they provide realistic results. Regression analysis-based statistical models are carried out using real dam failure data and estimating the parameters, which is achieved by characterizing the breach development as a function of other dam and reservoir characteristics (Zhu et al. 2004; Peter et al. 2018; Zhong et al. 2020).

3 Study Area and Data

Atasu Dam is in eastern Turkey in Trabzon Province, which is located between 38° 30 ′—40° 30 ′ east longitudes and 40° 30 ′—41° 30 north latitudes. It is situated on the Galyan Stream in Maçka Town, and it is connected to the city center via Değirmendere Stream. Atasu Dam is a concrete-paved, rock fill-type dam, and it is equipped with a lateral spillway on the right bank. The total effective crest length of the spillway is 90 m with a

Table 1 Specifications of Atasu Dam

Physical parameter	Unit	Value
Thalweg level	m	206.50
Foundation level	m	202.55
Crest elevation	m	320.55
Crest length	m	372.26
Crest width	m	7.8
Dam height from the foundation	m	118
Dam height from the thalweg	m	116
Total reservoir volume at normal water level	hm^3	35.75
Total reservoir volume at maximum water level	hm^3	37.87
Total reservoir volume at catastrophic water level	hm^3	39.11

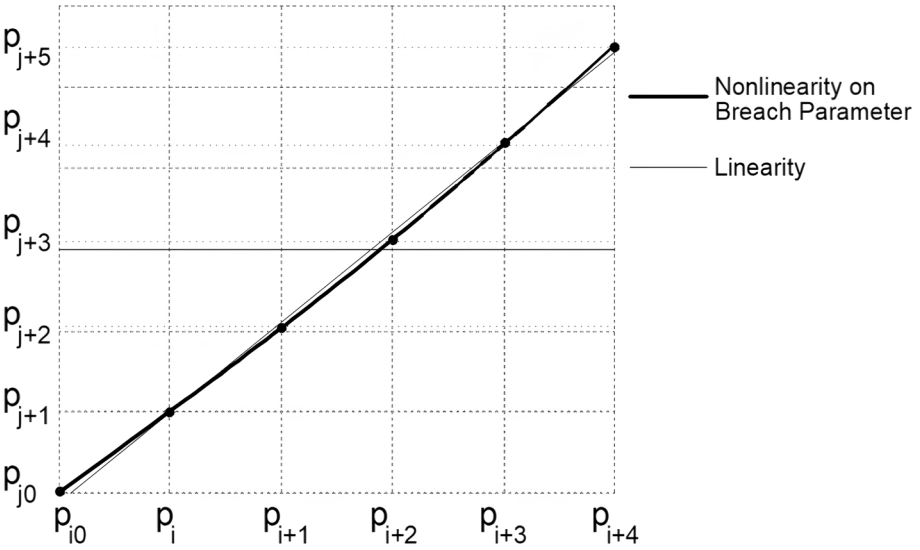

Fig. 1 Nonlinearity on the breach parameters

discharge capacity of 745.50 m^3/s (Marangoz and Anılan 2022). A list of features of Atasu Dam is presented in Table 1.

4 Method

In this study, six of the most effective dam failure parameters i.e., the left–right slope, breach weir coefficient, breach formation time, final bottom width, final bottom elevation, and initial elevation were continuously increased at certain rates, and the effects of these increments on the breach flow and time to reach the peak were assessed. In Fig. 1, p_i and p_j represent the amount of the increment and the tested failure model, respectively. Nonlinearity was obtained through the increments of parameters at a parabolic curve. Unlike linearity, a nonlinearity is obtained by increasing parameters at logarithmic rates.

In the figure, p_{i0} represents the unit state of the parameters, p_i shows the value that was increased by 5%, and p_{i+1} shows the value of p_i that was increased by 5%. Each of the expressions, p_{j0}, p_j, $p_{j+1}\ldots$ p_{j+5}, show the increment results of the ambiguous parameters that were considered in dam failure. In this way, 5 models were obtained by increasing the initial value of each of the 6 parameters by 5% compared to their previous numerical values. While each of the parameters were increased, the others were kept constant. In this way, only the independent effects of the relevant failure parameter properties on the breach could be observed. A bold parabolic curve was the considered ambiguous parameter itself. Each parameter can be expressed as in the following:

$$p_{(i0)} = f_{(p(j0))}, p_i = f_{(p(j+1))}, p_{(i+1)} = f_{(p(j+2))}, p_{(i+2)} = f_{(p(j+3))}, p_{(i+3)} = f_{(p(j+4))}, p_{(i+4)} = f_{(p(j+5))}$$

The selected parameter increments, and initial values were in compliance with Froehlich's (1995b) empirical breach formation system, which is shown in Eq. (1) and Eq. (2):

$$B_{ave} = 0.1803 * K_0 * V_w^{0.32} * h_b^{0.19} \tag{1}$$

$$t_f = 0.00254 * V_W^{0.53} * h_b^{-0.9} \tag{2}$$

Here B_{ave}: average breach width (m), V_w: reservoir water volume which is above the breach bottom in the moment of failure (m^3), h_b: total breach height. K_0 can be taken as 1.4 in the case of overtopping. The duration which is between the failure of the dam and the breach reaching its final form is defined as t_f.

4.1 The Outflow Hydrograph and Stage Headwater of Breach Shape on the Dam Axis

The flow through the dam axis was equal to the sum of the flow over the crest of the dam, the flow through the breach, and the flow through the spillway and bottom weir of the dam (Eq. 3).

$$Q_T = Q_O + Q_b + Q_{dis} + Q_{dos} \tag{3}$$

Here Q_T shows the flow through the dam axis at a certain time t during dam failure, Q_o shows the flow over the crest of the dam, Q_b shows the flow through the breach, while Q_{dis} and Q_{dos} show the flows through the spillway and bottom weirs of the dam, respectively. In dams where the spillway is above the body of the dam, the flow through the spillway can be included in the flow over the crest of the dam. The flow through the bottom weir can be expressed with the orifice flow. However, it can be neglected if it is thought that the bottom weirs are closed during the failure, or if the flow through the bottom weir is negligible when compared to other flow expressions. In this way the expression $Q_T=Q_O+Q_b$ can be simplified as the sum of the flows over the crest and through the breach. Harris and Wagner (1967) and Brown Richard and Rogers (1981), in their studies, expressed the flow over the dam with the physical model they developed. Accordingly, the total flow through the dam axis can be obtained by the following equation (Eq. 4):

$$Q_O = \left(gA^3W^{-1}\right)^{0.5} \tag{4}$$

here, W: crest length (m), A: cross-section of the flow over the crest, (m^2), g: gravitational acceleration. Cross-sectional area of the flow over the crest, on the other hand, can be calculated using the following equation (Eq. 5):

$$A = Wy_c \tag{5}$$

Here, y_c is the height of the critical flow over the crest (m). This value is expressed as 75% of the difference between free water surface h(t) and the crest elevation z(t) (Eq. 6):

$$y_c = 0.75(h(t) - z(t)) \tag{6}$$

If (Eq. 4) and (Eq. 5) are written in the equation (Eq. 6);

$$Q_O = 3.68W(h(t) - z(t))^{1.5} \tag{7}$$

(Eq. 7) expression can be obtained. According to the physical model produced by Singh and Scarlatos (1987) and developed by Singh and Quiroga (1987), the flow through the breach in the body of the dam can be expressed using the following (Eq. 8):

$$Q_b = Q_{ü} + Q_d \tag{8}$$

here; $Q_{ü}$ represents the total flow through the breach for trapezoidal breach assumption in an earthfill dam where the breach is formed with overtopping, while Q_d stands for the flow through the triangular or rectangular breach. In obtaining the breach flow (with the assumption that it is in consistency with the wide-crested weir model), rectangular and triangular breach calculations are made in the case of a trapezoidal breach and the values obtained are summed (Eq. 9). Accordingly.

$$Q_b = Q_{ü} + Q_d = C_d C_t b(y_b(t))^{2.5} + C_d C_r b(y_b(t))^{1.5} \tag{9}$$

where C_d is the discharge coefficient, b is the breach bottom, C_t is the discharge coefficient for the triangular section ($\sqrt{m}/s$) and C_r is the discharge coefficient for the rectangular section ($\sqrt{m}/s$). If the effects of the tailwater are to be considered, Q_b must be modified (Singh 1996). However, in this study, the tailwater was not considered. In the following equation, h_d is the height of the dam, y is the water height in the main channel z_2, h_2 is top of the breach and the water load on dam axis during the failure at ''t'' time, and D is the distance between the bottom of the breach and crest:

$$\frac{y + h_d - D}{h_2(t) - z_2(t)} > 0.67 \tag{10}$$

in the case where the expression above is valid, a correction of Q_b value is made. The flow hydrograph was obtained by calculating the flow rates Q_o and Q_b for each time step. For this, the change in water must be expressed in terms of height and should be considered in the upstream side. In the case where the (Eq. 10) expression is not valid, then it can clearly be said that the Q_b flow is not affected by the tailwater.

4.2 Management of the Breach Parameters

Each of the 6 dam failure parameters were increased in an order and their effects on the dam failure were investigated. Increments of 5% compared to the previous value were implemented five times. The reasons for the selection of a ± 5% increment method was due to the investigation of the parameter effects of the dam failure and in being able to create a scenario within a confidence interval. In this way, 36 dam failure scenarios were examined. Despite the changing parameters, the other 5 parameters were kept constant at their initial values. Fixed values

were determined in accordance with Froehlich (1995a) dam breach acceptance. In addition, the ranges of possible values for breach characteristics (USACE 2016) and the values between the minimum and maximum numerical values of any parameter were designed in accordance with the dam (Table 2). Breaches are formed as a result of the failure of the dam in expanding in time and overcoming its final form. In this study, the shape of the breach was accepted as a trapezoidal section. In all cases, the mode of failure was overtopping.

4.2.1 Breach Side Slopes

Although a breach on the dam body does not have to have a specific geometric shape in a real dam failure, it was assumed to have a specific geometric shape in order to facilitate mathematical expression and to be able to predict breach formation. The shape of the breach was due to the initiation of the dam failure being assumed as trapezoidal in this study. Breach formation was again assumed as trapezoidal. The right and left side slopes of the resulting trapezoidal cross-section were influential in determining the flow resulting from the dam failure. Accordingly, it was assumed that they are equal, and the right and left side slopes were modified, as shown in Table 3. In this way, while the breach side slope takes a value of 1.2 in the first scenario, the other values were taken as 1.26, 1.32, 1.39, 1.46, and 1.53, respectively, and the first six scenarios were thus completed. The left–right slope, also termed the breach side slope, can be explained as the horizontal distance to the 1-step vertical distance. Since the first value was selected as 1.39 for the left–right slopes, this value was kept constant in all parameter increments.

4.2.2 The Breach Weir Coefficient

The breach weir coefficient parameter changes the outlet hydrograph by directly affecting the flow through the breach after breach formation. Unfortunately, the exact knowledge of the magnitude of these coefficients for a dam failure (either by overtopping or piping failure) is not known. There are many approaches for obtaining the breach weir coefficient parameter, but this situation might not be valid for every dam type. However, the same coefficients are often used when calculating the physical properties of a flood wave overtopping a dam or passing through a weir.

These coefficients can be evaluated according to two different types of weirs. First, a typical sharp-crested weir problem is solved to estimate the breach flow, which occurs when the water in the dam reservoir continuously cuts the dam body like an arrow. However, earthen dams with medium-to-very-large storage volumes upstream will most likely have failed all the way down to the natural stream bed elevation; thus, they will be in the breach widening phase when the peak outflow occurs. This would suggest the use of a weir coefficient (C) that is typical of a broad-crested weir with a long crest length. A broad-crested weir problem can be solved via the calculation of the flow through a trapezoidal breach or flow overtopping a dam body that is eroded up to halfway. Trapezoidal weir side slopes that are known can be modeled using the following equation (Eq. 11):

$$Q = 0.4CZH^{2.5} \tag{11}$$

here, Q: discharge over side-sloped portion of weir (cm/s), Z: side slope (Z horizontal to 1 vertical) of the weir crest, H: distance between water surface and the crest (m), C: weir coefficient, typically between 1.1 to 1.8 for earthfill dam on Metric System.

Table 2 Ranges of possible values for breach characteristics (USACE 2016)

Dam type	Average breach width B_{ave}	Horizontal component of breach side slope (H) H:1 V	Failure time T_f (hrs)	Agency
Earthen/ Rockfill	(0.5 to 3.0) x HD	0 to 1.0	0.5 to 4.0	COE 1980
	(1.0 to 5.0) x HD	0 to 1.0	0.1 to 1.0	FERC
	(2.0 to 5.0) x HD	0 to 1.0 (Slightly larger)	0.1 to 1.0	NWS
	(0.5 to 5.0) x HD*	0 to 1.0	0.1 to 4.0*	COE 2007

*where: HD: height of the dam

** Dams that have very large volumes of water, and have long dam crest lengths, will continue to erode for long durations (i.e. as long as a significant amount of water is flowing through the breach), and may therefore have longer breach widths and times than what is shown in table

Table 3 Breach parameter values for different cases

Parameters	Cases					
	1	2	3	4	5	6
Breach side slope	1,20	1,26	1,32	1,39**	1,46	1,53
Breach weir coefficient	1,4**	1,47	1,54	1,62	1,7	1,79
Breach development time	0,51**	0,49	0,46	0,44	0,42	0,4
Final bottom width	42**	44,10	46,31	48,62	51,05	53,60
Final bottom elevation	306,31	291,72	277,83	264,60	252,00	240**
Initial elevation of reservoir	248,00	260,40	273,42	287,09	301,45	316.5**

** represents default value for other cases

The numerical values of the breach weir coefficient used in the calculations are presented in Table 3. The breach weir coefficient was taken as 1.4 in the first scenario, and then as 1.47, 1.54, 1.62, 1.70, and 1.79 in the other five scenarios, respectively. As such, the first six scenarios were completed in this way. Since the initial value for this ambiguous parameter was taken as 1.4, the first value was kept constant for all the other parameter increments.

4.2.3 Breach Formation Time

Since the velocity in the dam reservoir was at its maximum at the center of the channel, the first breach openness in the dam mostly took place in the middle of the dam and continued to form as long as the upstream flow permitted, up until the bottom border of the breach became visible. Sometimes this border was equal to the dam height, while in other cases it formed independent of that height. Still, the volume of the reservoir was found to be effective in this formation mechanism. In Fig. 2, a scheme of a breach formation, which is from the middle of the dam crest down to a certain amount below, is shown. Accordingly, after 0.51 h, the deformation of the dam body caused by the water remaining in the reservoir was limited. Therefore, this period was referred to as the breach formation time or breach development time.

All the parameters are shown in Table 3. The breach development time parameter was taken as 0.40 in the first scenario, and was then taken as 0.42, 0.44, 0.46, 0.49, and 0.51 in the other five scenarios, respectively. When the increments were implemented with other ambiguous parameters, the initial value of the breach development parameter was taken as 0.51.

The first value was taken as 0.51 for the breach development time (hrs), and this was then taken as 0.42, 0.44, 0.46, 0.49, and 0.51 h in the other five scenarios, respectively; as such, the first six scenarios were completed in this manner. Since the initial value for this ambiguous parameter was chosen as 0.51, this value was kept constant for all parameter increments.

4.2.4 Final Bottom Width

The final bottom width B_f refers to the state when there is no more water to sluice, and the final breach is formed in the body where the failure takes place. The final bottom width when there is overtopping in the case of the formation of a trapezoidal breach can be expressed as per the following (Fig. 3):

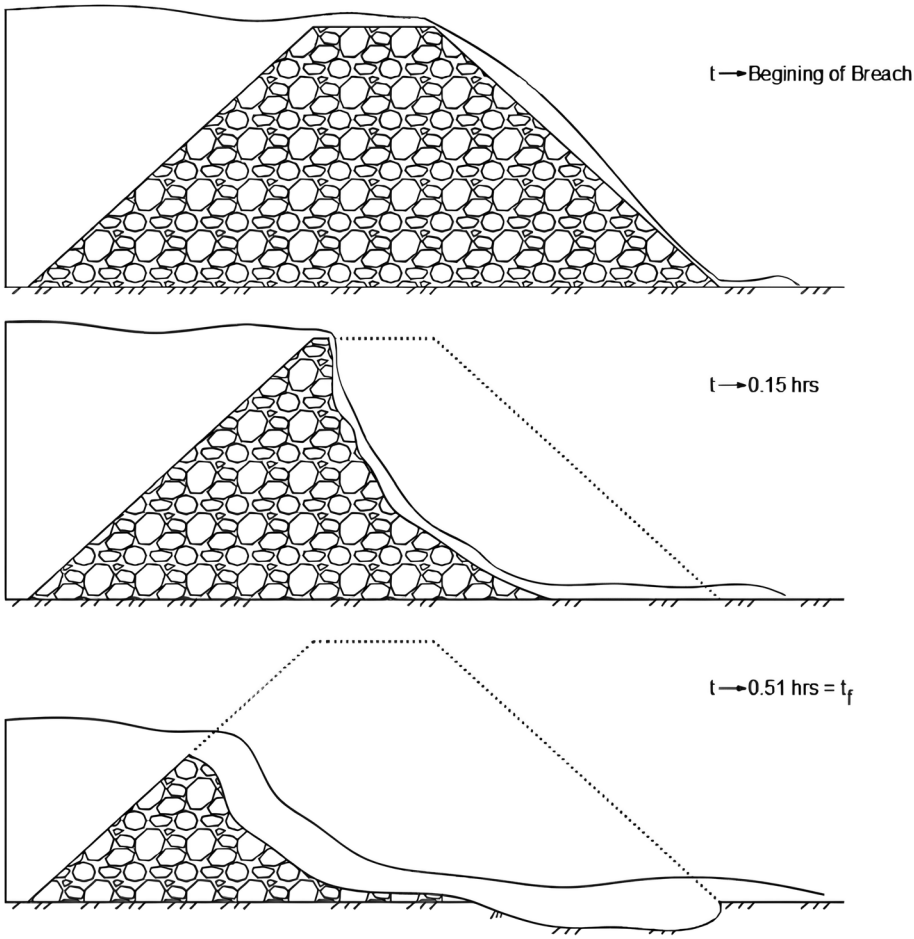

Fig. 2 Dam break formation scheme on perpendicular axis

$$B_f = B_{ave} - 2 * Mb * (Cr_e - Bf_e) \tag{12}$$

here; B_f,: final breach width, B_{ave}: average breach width, Mb: lateral breaking slope of the breach (horizontal/vertical), Cr_e and Bf_e: elevation of the crest and final breach bottom, respectively. B_{ave} can be obtained using any of the breach formation estimation methods.

The first 6 scenarios were completed by taking values of 44.1, 46.31, 48.62, 51.05 and 53.60, respectively, for the final bottom width, while 42 m was taken in the first scenario. Since the initial value of 42 m was chosen for this uncertain parameter, the relevant value was kept constant in all parameter increments.

4.2.5 Final Bottom Elevation

The final bottom elevation is one of the vaguest parameters among all breach parameters. It implies the end level of the breach. Certain cases have shown that the final bottom elevation

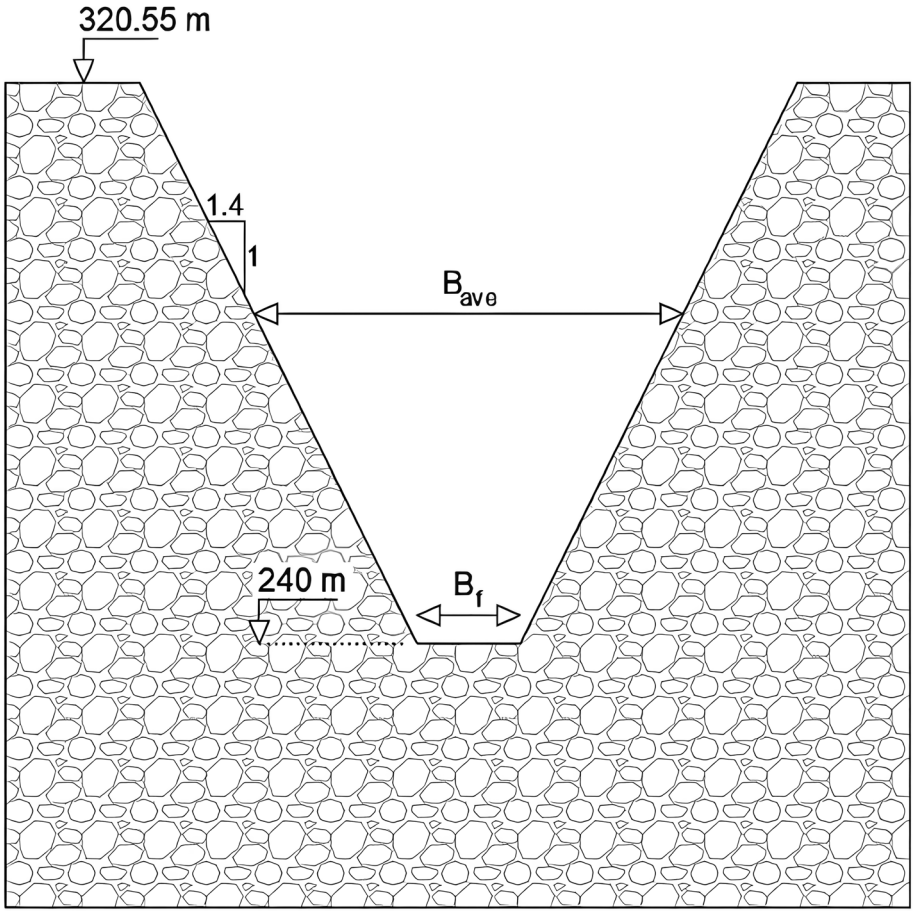

Fig. 3 Formation of a trapezoidal breach in case of overtopping

completely matches the base or talweg elevation; however, it can also be half height of the dam. Technically there is no adequate prediction type for this parameter. Breaches occur in solid parts on concrete dams as per the USACE (1980) assumption. However, gradual breaching has been observed in earthen/fill dams as per FERC (1988).

For the final bottom elevation, 306.31 m was taken for the first scenario, while 291.72, 277.83, 264.60, 252, and 240 were taken for the other 5 scenarios, respectively, thus completing the first 6 scenarios. Since the initial value for this ambiguous parameter was chosen as 240 m, the value then remained constant for all parameter increments.

4.2.6 Initial Elevation of the Reservoir

Although the upper water elevation value of the dam reservoir during the failure was not theoretically accepted as a breach parameter, it still directly affected the breach formation mechanism. Since there is a difference between the upper elevation of the reservoir water and the construction foundation in dams constructed in narrow valleys, the effects of this ambiguous parameter can be amplified. However, in arid or particularly rainy regions or in

regions where the reservoir water is suitable for the transmission of electricity, irrigation, and distribution lines the upper levels of reservoir water can vary considerably. Of course, if this value is high, it would cause an expansion in the borders of the breach, which would be formed because of dam failure and the openness of the body increasing at a higher rate. Nevertheless, the cumulative effect of the change in the reservoir water elevation with respect to dam failure needs to be obtained along with other ambiguous parameters.

The initial water elevation, or initial water level, parameter of the dam reservoir during the dam break was first chosen as 248 m. It was then selected as 260.40, 273.42, 287.09, 301.445, and 316.50 m for the other five scenarios, respectively. The normal water level under the dam's operating conditions was 316.50 m, and it was selected as the initial value for this parameter while the other ambiguous parameters were being tested. Due to the fact that today's dams are continuously monitored electronically, unlike in the past, and as water levels are monitored both on the upstream and downstream sides, this parameter is easier to establish and predict than other parameters. Nevertheless, extraordinary cases might cause the initial water level of the reservoir to change and thus prevent it from being known.

5 Results

The six ambiguous parameters examined in this study were tested for six scenarios that were created for each of them and their respective effectiveness were investigated. Accordingly, the amount of contribution to the maximum and average flow, as well as the maximum and average times required to reach the peak flow, were considered.

5.1 Parameter Efficiency on the Breach Peak Flow

Within the scope of the 36 dam failure scenarios that were planned systematically, the failure hydrographs that occurred at the dam axis were obtained and the peak discharge values of these hydrographs were recorded. Accordingly, the peak flow at the dam axis with respect to the lowest and highest parameter values for each parameter was evaluated (Fig. 4). Moreover, regarding the six scenarios formed for each parameter, a comparison of the peak discharges based on the increment rates was also conducted (Fig. 5).

Accordingly, the side slope parameter caused an increment of 440 m^3/s in the peak discharge value from the first scenario to the very last. In this way, it caused a total 1.84% increment in the peak discharge. Similarly, the peak discharge difference with respect to the breach weir coefficient parameter at the limit values was an increment of 693 m^3/s, which was determined to be a 2.84% increase. The peak flow difference at the limit values with respect to the breach development time parameter was 5700 m^3/s. This value resulted in an increase of 18.98%. The peak flow difference at the limit values with respect to the final bottom width parameter was 1412 m^3/s, which corresponded to an increase of 5.8%. The flow increase caused by the final bottom elevation parameter compared to the first and last parameter was 22,786 m^3/s, which was expressed as 1450% in percentage terms. This increase can also be expressed as a discharge increase of 23,000 m^3/s in the initial water elevation parameter, thus resulting in an increase of 1694.2%. It was observed that the initial bottom elevation and initial water elevation parameters exceeded 100% of the initial value, and thus increased by approximately 16 and 18 times, respectively, compared to their initial values.

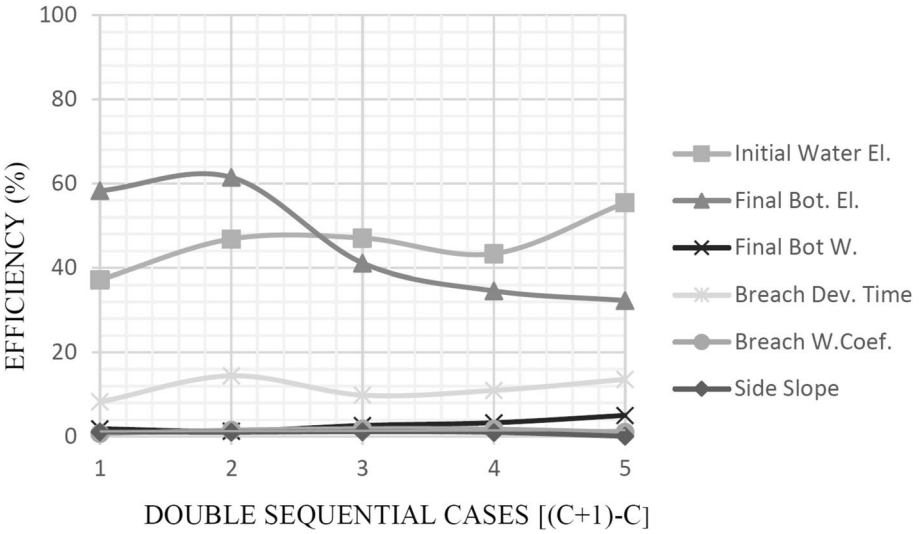

Fig. 4 Efficiency on peak flows of breach parameters for all cases

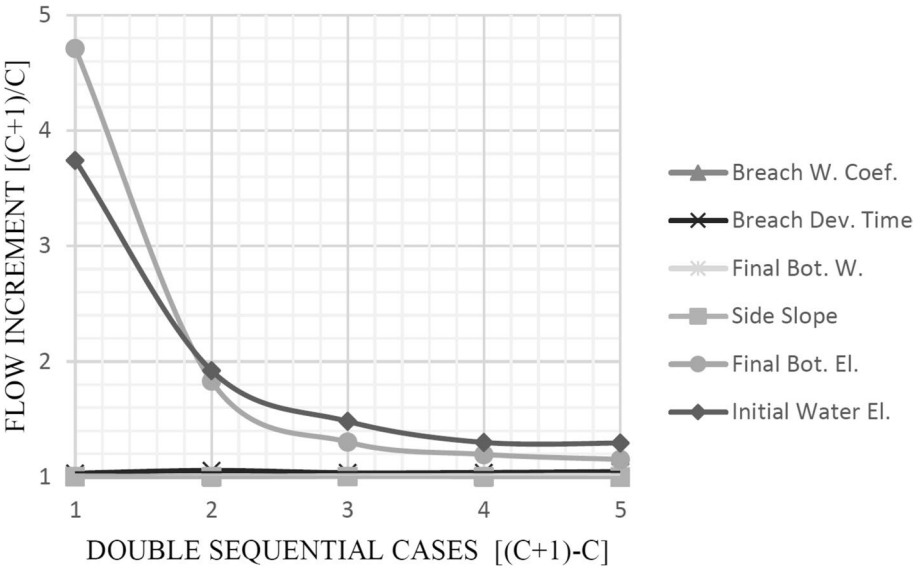

Fig. 5 Average parameter efficiency on peak flow

The average parameter efficiency was calculated by taking the pairwise differences for the consecutive scenarios between the maximum flow values obtained. Accordingly, the average increase per scenario was calculated. While the average increase in peak flows for the side slope parameter was around 0.37%; the average increase due to the breach weir coefficient parameter was 0.57%; the average increase due to the breach development value was 3.8%; the average increase due to final bottom width parameter was 1.16%; the average peak

discharge increase due to the final bottom elevation was 290.01%; and, finally, the average peak discharge increase due to initial the water elevation was 338%.

5.2 Parameter Efficiency on Time to Peak

The failure hydrographs that occurred at the dam axis, within the scope of the 36 dam failure scenarios that had been planned systematically, were obtained. In addition, the peak discharge values of these hydrographs were recorded (Fig. 6). For each parameter, the effects of the parameters on the peak times were analyzed by taking the maximum peak time differences based on the initial value (Fig. 7).

When the differences in the maximum peak reaching times between the initial and final values of the parameters were examined, it was observed that the peak discharge reaching times were the same for all values of the side slope parameter and that no change was observed. For the breach weir coefficient parameter, there was an average decrease of 0.47% and a maximum decrease of 2.35% in the time to reach the peak discharge from the initial value to the final value. In other words, the increment of this coefficient caused the flow from the dam failure to be discharged faster. From the initial value to the final value of the breach development time parameter, the time to reach the peak increased by a maximum of 4.94% and an average of 0.99%. The increase in the final bottom width value, according to the scenarios, decreased the time for the flow to reach the peak by a maximum of 4.71% and an average of 0.94% compared to the first case. In the scenario where the final bottom elevation value was from high to low, the time to reach the peak decreased by a maximum of 5.56% and an average of 1.11%. Finally, an increase in the initial water elevation parameter resulted in a decrease in the flow by a maximum of 6.59% and by 1.32% on average. The average efficiency percentages of the peak reaching times, which

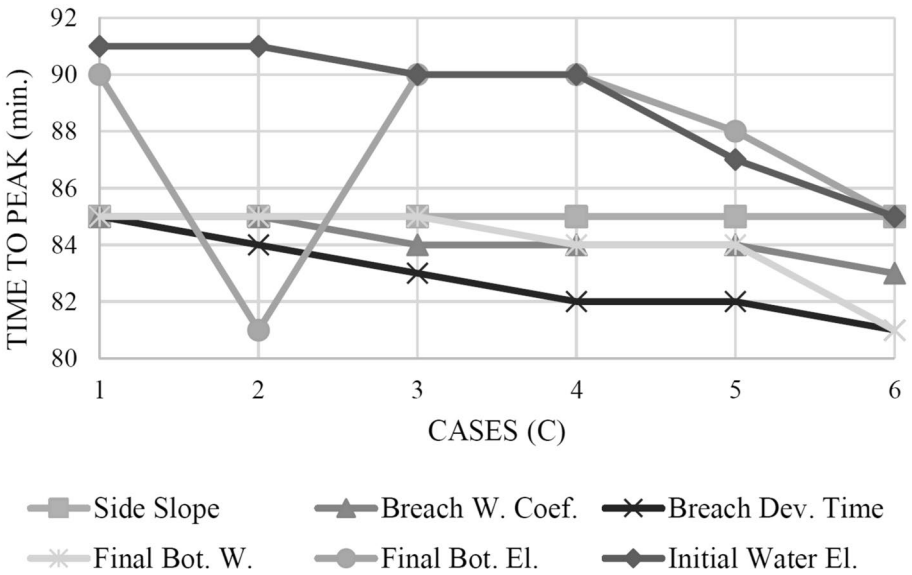

Fig. 6 Max. parameter efficiency on reach time to peak

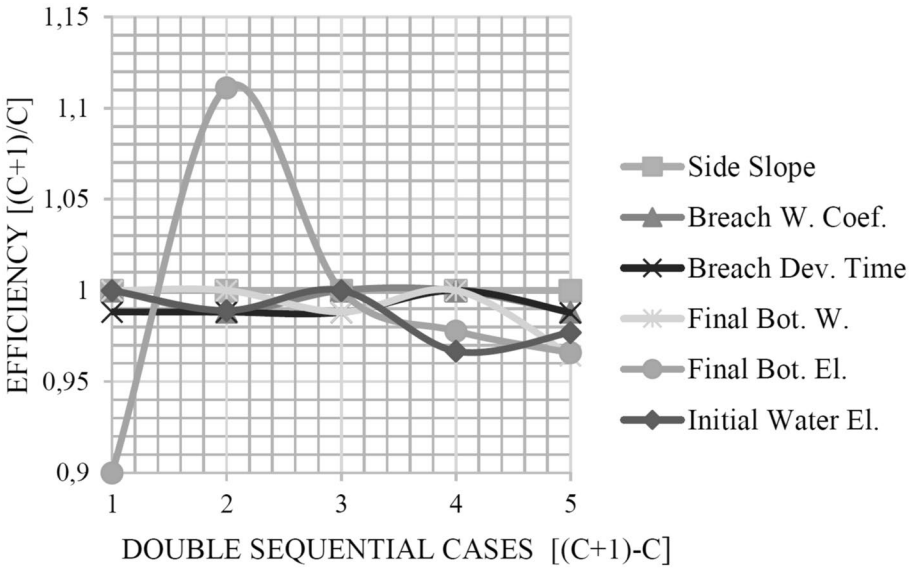

Fig. 7 Average parameter efficiency on reach time to peak

were obtained by averaging the differences between the consecutive parameters of the peak flow reaching times of the failure waves after dam failure, are shown below.

6 Discussion

Certain studies have focused on determining the sensitivity of parameter/model approaches by performing a sensitivity analysis (Li et al. 2021; Najar and Gül 2022). Our research revealed the critical importance, expressed in percentages, for any parameter that can be varied under a different perspective. Unlike previous research, a set of scenarios that has realistic and large-scale frequencies are preferred rather than those established via uncertainty analysis. Each parameter is tested with a reasonable case scenario under a real analytic equation set, which is a fact that was already proven by Froehlich (1995b) for most dam break studies.

Our research was compared with the study of Basheer et al. (2017), who investigated the influence of the dam parameter for Mosul Dam. In total, four uncertain parameters (i.e., the breach width, initial elevation of the reservoir, breach side slope, breach development (formation) time parameters) were considered in that research unlike our six parameters. They carried out a standard sensitivity analysis to establish the trend of the parameters. However, we did not use a sensitivity analysis that consists of certain fixed percentage and arbitrary values as they produce unrealistic results for each value. Instead of that type of approach, we highly recommend a physical-based empirical solution with a significant number of cases for a specified dam interest. Thus, all the cases and scenarios refer to a real probability. Moreover, we also recommend this new approach for its superiority in determining parameter effectiveness. The 5% increment in each scenario caused a non-linearity that never overlapped nor repeated with the previous one. Basheer preferred a 1D, cross-sectional-based topography. Our research consists of a domain that includes the dam reservoir and dam only. This means that the direct flow output after a sudden dam break under certain scenarios can be shown and calculated properly.

A limitation in dam break parameter analysis is its validation. However, validation opportunities are limited since actual dam break cases are rare and observation data are sparse (Rizzo et al. 2023). Moreover, the conclusions established in this investigation are specific to the study site analyzed; thus, they specifically correspond to the Atasu Dam. However, the methodology could be adapted and replicated in other reservoirs of interest, and thus could determine whether the behavior is similar to that presented in this study. More research would also be useful for the same study area. A physical-based basin model that covers the city center and includes bridges and flood protection structures up to the point where the river meets the sea may be useful. Moreover, a comparison laboratory scale model that uses the same approach of our research and mathematical model would be useful for showing an effective case study with higher accuracy. It would also be advantageous to evaluate downstream floods that are related to dam break parameters. Furthermore, a dam breach analysis could be performed using artificial intelligence models or three-dimensional CFD models (Kyaw and Uchida 2023). A higher level of assessment could also be provided through a probabilistic method based on a set of potential dam break scenarios, like Rizzo et al. (2023) performed in their studies.

7 Conclusions

In a dam failure event, uncertainty in the dam breach parameters would mean that the size of the disaster cannot be fully determined. The characteristics of the flood hydrographs resulting from a dam breach essentially depend on the breach parameters. The effectiveness of the parameters that will directly affect the formation of the peak flow that will occur in a dam failure is particularly important. Therefore, understanding the breach mechanism is an essential task for the design of flood mitigation, flood mapping, and flood warning systems.

In this paper, a comprehensive method for determining the efficiency of dam break parameters was used for failure scenarios regarding a specific dam. To understand the impact of the breach parameters on flood peak hydrographs and time to reach the peak, 6 of the most common breach parameters were selected and 36 scenarios were examined. These scenarios were tested based on the occurrence of the peak flow from the dam breach and the time to reach the peak. According to the findings, the most effective parameters were, respectively, the initial water elevation, final bottom elevation, and breach development time. Thus, by using the most popular physical breach model, the dam break parameters were shown and sorted by critical importance. Based on the results of the study, we are able to state the following conclusions:

- The method aids in determining how to interpret possible flood risks due to dam break;
- An initial operational action saves time during any adverse conditions.

The obtained results presented in this paper can provide identifying parameters whose effectiveness is essential for dam break analysis. Determining which parameters are the most critical and which ones are negligible would be useful for decision makers in terms of establishing evacuation and risk management procedures.

Author Contributions All authors contributed to the study conception and design. Material preparation, data collection and analysis were performed by H O. Marangoz. The first draft of the manuscript was written by T Anılan. S Karasu discussed the results and contributed to the final text and commented on previous versions of the manuscript. All authors read and approved the final manuscript.

Funding Open access funding provided by the Scientific and Technological Research Council of Türkiye (TÜBİTAK). The authors declare that no funds, grants, or other support were received during the preparation of this manuscript.

Data Availability Data and models that support the findings of this study are available from the corresponding author upon reasonable request.

Declarations

Competing Interests The authors have no relevant financial or non-financial interests to disclose.

References

Anılan T, Yüksek Ö (2017) Perception of flood risk and mitigation: survey results from the Eastern Black Sea Basin. Turkey Nat Hazard Rev 18(2):05016006

Basheer TA, Wayayok A, Yusuf B, Kamal MR (2017) Dam breach parameters and their influence on flood hydrographs for Mosul Dam. J Eng Sci Technol 12(11):2896–2908

Bello D, Alcayaga H, Caamaño D, Pizarro A (2022) Influence of dam breach parameter statistical definition on resulting rupture maximum discharge. Water 14(11):1776

Bellos V, Tsakiris VK, Kopsiaftis G, Tsakiris G (2020) Propagating dam breach parametric uncertainty in a river reach using the HEC-RAS software. Hydrol 7(4):72

Brown Richard J, Rogers DC (1981) User's Manual for Program BRDAM, U.S. Bureau of Reclamation, Denver, Colorado, pp 73

FERC (1988) Notice of revised emergency action plan guidelines. USA Federal Regulatory Commission. Washington, pp 31

Froehlich DC (1995a) Embankment dam breach parameters revisited. Proceedings, water resources engineering, 1995 ASCE conference on water resources engineering. ASCE, New York, pp 887–889

Froehlich DC (1995b) Peak outflow from breached embankment dam. J Water Resour Plann Manage 121(1):90–97

Froehlich DC (2008) Embankment dam breach parameters and their uncertainties. J Hydraul Eng 134(12):1708–1721

Garoosi F, Mellado-Cusicahua AN, Shademani M, Shakibaeinia A (2022) Experimental and numerical investigations of dam break flow over dry and wet beds. Int J Mech Sci 215:106946

Haltaş I, Tayfur G, Elçi S (2016) Two-dimensional numerical modeling of flood wave propagation in an urban area due to Ürkmez Dam-Break, İzmir. Turkey Nat Hazard 81(3):2103–2119

Harris GW, Wagner DA (1967) Outflow from breached earth dams. Thesis, presented to the Univ. of Utah, at Salt Lake City, Utah, in partial fulfillment of the requirements for the degree of Bachelor of Science, pp 102

Karim IR, Hassan ZF, Abdullah HH, Alwan IA (2021) 2D-HEC-RAS modeling of flood wave propagation in a semi-arid area due to dam overtopping failure. Civil Eng J 7(9):1501–1514

Khoshkonesh A, Sadeghi SH, Gohari S, Karimpour S, Oodi S, Di Francesco S (2023) Study of dam-break flow over a vegetated channel with and without a drop. Wat Resour Manage 37(5):2107–2123

Kyaw PPSS, Uchida T (2023) Assessment of the Breaching Event, Breach Parameters and Failure Mechanisms of the Spillway Collapse in the Swa Dam. Myanmar Water 15(8):1513

Lee KH (2019) Simulation of dam-breach outflow hydrographs using water level variations. Wat Resour Manag 33(11):3781–3797

Li C, Gao H, Xu Z, Huang Y (2021) Sensitivity analysis of rock-fill dam break flood on different dam break durations. Open J Saf Sci and Technol 11(3):89–103

Liu Z, Xu X, Cheng J, Wen T, Niu J (2018) Hydrological risk analysis of dam overtopping using bivariate statistical approach: a case study from Geheyan Reservoir. China Stochastic Environ Res Risk Assess 32(9):2515–2525
Marangoz HO, Anılan T (2022) Two-dimensional modeling of flood wave propagation in residential areas after a dam break with application of diffusive and dynamic wave approaches. Nat Hazard 110(1):429–449
Najar M, Gül Ali (2022) Investigating the influence of dam-breach parameters on dam-break connected flood hydrograph. UCTEA- Turk Chaber Civil Eng- Tech J 33(5):12501
Özmen-Çağatay H, Turhan E, Kocaman S (2022) An experimental investigation of dam-break induced flood waves for different density fluids. Ocean Eng 243:110227
Peng L, Zhang T, Rong Y, Hu C, Feng P (2021) Numerical investigation of the impact of a dam-break induced flood on a structure. Ocean Eng 223:108669
Peng L, Zhang T, Li J, Feng P (2023) Three-dimensional numerical study of dam-break flood impacting problem with VOF method and different turbulence closures. Wat Resour Manage 37:1–21
Peter SJ, Siviglia A, Nagel J, Marelli S, Boes RM, Vetsch D, Sudret B (2018) Development of probabilistic dam breach model using Bayesian inference. Water Resour Res 54(7):4376–4400
Psomiadis E, Tomanis L, Kavvadias A, Soulis KX, Charizopoulos N, Michas S (2021) Potential dam breach analysis and flood wave risk assessment using HEC-RAS and remote sensing data: a multicriteria approach. Water 13(3):364
Ramola M, Nayak PC, Venkatesh B, Thomas T (2021) Dam break analysis using Hec-Ras and flood inundation modelling for Pulichinatala Dam in Andhra Pradesh. India Indian J of Ecol 48(2):620–626
Říha J, Kotaška S, Petrula L (2020) Dam break modeling in a cascade of small earthen dams: case study of the Čižina River in the Czech Republic. Water 12(8):2309
Rizzo C, Maranzoni A, D'Oria M (2023) Probabilistic mapping and sensitivity assessment of dam-break flood hazard. Hydrolog Sci J 68(5):700–718
Sarchani S, Koutroulis AG (2022) Probabilistic Dam breach flood modeling: the case of Valsamiotis Dam in Crete. Nat Hazard 114:1–52
Shen G, Sheng J, Xiang Y, Zhong Q, Yang D (2020) Numerical modeling of overtopping-induced breach of landslide dams. Nat Hazard Rev 21(2):04020002
Singh VP, Scarlatos PD (1987) Modeling of gradual earthfill dam erosion In: Balasubramaniam AS, Chandra S, Bergado DT, Nutalaya P (eds) Environmental geotechnics and problematic soils and rocks. CRC Press, pp 129–138
Singh VP, Quiroga CA (1987) A dam-breach erosion model: I. formulation. Water Resour Manage 1:177–197
Singh VP (1996) Dam breach modelling technology. Kluwer academic publishers, pp 244
Tingsanchali T, Chinnarasri C (2001) Numerical modelling of dam failure due to flow overtopping. Hydrol Sci J 46(1):113–130
Turhan E, Özmen-Çağatay H, Kocaman S (2019) Experimental and numerical investigation of shock wave propagation due to dam-break over wet channel. Pol J Environ Stud 28(6):1–24
USACE (1980) Flood emergency plans. ''Guidelines for corps dams'' (version RD-13, June). California, pp 62
USACE (2016) HEC-RAS river analysis system. ''User's manual'' (version CPD-69, February). Institute for water resources, California, pp 960
Wahl TL (2010) Dam breach modeling–an overview of analysis methods. In Joint federal interagency conference on sedimentation and hydrologic modeling, vol 27
Wang B, Yang S, Chen C (2022) Landslide dam breaching and outburst floods: a numerical model and its application. J Hydrol 609:127733
Yi X (2011) A dam break analysis using HEC-RAS. J Water Resour Protect 3(6):370–379. https://doi.org/10.4236/jwarp.2011.36047
Yudianto D, Ginting BM, Sanjaya S, Rusli SR, Wicaksono A (2021) A framework of dam-break hazard risk mapping for a data-sparse region in Indonesia. ISPRS Int J Geo-Inf 10(3):110
Zali N, Molaei Hashjin N, Taghizadeh S (2021) Regional planning approach to protect surrounding towns and villages in the event of dam break: case study of AchChay Dam. Nat Hazard Rev 22(4):05021013
Zhang S, Tan Y (2014) Risk assessment of earth dam overtopping and its application research. Nat Hazard 74(2):717–736
Zhong Q, Chen S, Fu Z, Shan Y (2020) New empirical model for breaching of earth-rock dams. Nat Hazard Rev 21(2):06020002
Zhu YH, Visser PJ, Vrijling JK (2004) Review on embankment dam breach modeling. New developments in dam engineering. Taylor & Francis Gr, London, UK, pp 1189–1196